Published in final edited form as:
J Immunol. 2014 March 15; 192(6): 2576–2584. doi:10.4049/jimmunol.1301857.

The DC-HIL/Syndecan-4 Pathway Regulates Autoimmune Responses Through Myeloid-derived Suppressor Cells

Jin-Sung Chung[*], **Kyoichi Tamura**[*,‡], **Hideo Akiyoshi**[*,†], **Ponciano D. Cruz Jr.**[*], and **Kiyoshi Ariizumi**[*]

[*] Department of Dermatology, The University of Texas Southwestern Medical Center and Dermatology Section (Medical Service), Dallas Veterans Affairs Medical Center, Dallas, TX.

Abstract

Having discovered that the DC-HIL receptor on antigen presenting cells inhibits T cell activation by binding to syndecan-4 (SD-4) on T cells, we hypothesized that the DC-HIL/SD-4 pathway may regulate autoimmune responses. Using experimental autoimmune encephalomyelitis (EAE) as a disease model, we noted an increase in SD-4^{+} T cells in lymphoid organs of wild-type (WT) mice immunized for EAE. The autoimmune disease was also more severely induced (clinically, histologically, and immunophenotypically) in mice knocked-out for SD-4 compared to WT cohorts. Moreover, infusion of SD-4$^{-/-}$ naive T cells during EAE induction into Rag2$^{-/-}$ mice also led to increased severity of EAE in these animals. Like SD-4 on T cells, DC-HIL expression was upregulated on myeloid cells during EAE induction, with CD11b^{+}Gr-1^{+} myeloid-derived suppressor cells (MDSC) as the most expanded population and most potent T cell suppressor among the myeloid cells examined. The critical role of DC-HIL was supported by DC-HIL gene deletion or anti-DC-HIL treatment, which abrogated MDSC's T cell suppressor activity and also by DC-HIL activation inducing MDSC expression of IFN-γ, nitric oxide, and reactive oxygen species. Akin to SD-4$^{-/-}$ mice, DC-HIL$^{-/-}$ mice manifested exacerbated EAE. Adoptive transfer of MDSC from EAE-affected WT mice into DC-HIL$^{-/-}$ mice reduced EAE severity to the level of EAE-immunized WT mice, an outcome that was precluded by depleting DC-HIL^{+} cells from the infused MDSC preparation. Our findings indicate that the DC-HIL/SD-4 pathway regulates autoimmune responses by mediating the T cell suppressor function of MDSC.

Introduction

Among the immune system's difficult tasks is to defend the host against microbial pathogens while controlling autoreactivity. Most autoreactive T cells are depleted (centrally) in the thymus during early development, but some escape this screening process (1) and will require suppression of their activation (peripherally) in order to maintain homeostasis. Cells responsible for peripheral tolerance include regulatory T cells (Treg), tolerogenic macrophages and dendritic cells (DC), and invariant natural killer (NK) T cells (2). A newly recognized player in this milieu are CD11b^{+}Gr-1^{+} myeloid-derived suppressor cells (MDSC) that can potently suppress T cell function as well as promote expansion of Treg (3, 4).

Correspondence: Kiyoshi Ariizumi Phone: 214-633-1835; Fax: 214-648-0280; Kiyoshi.Ariizumi@UTSouthwestern.edu.
[†]Current address: Department of Veterinary Science, Graduate School of Life and Environmental Sciences, Osaka Prefecture University, Osaka, Japan
[‡]Current address: Department of Veterinary Internal Medicine, Faculty of Veterinary Medicine, Nippon Veterinary and Life Science University, Tokyo, Japan

Disclosures
The authors have no financial conflicts of interest.

T cell activation is regulated by costimulatory and coinhibitory ligand and receptor pairs of molecules expressed on T cells and APC, respectively. The coinhibitory limb includes CTLA-4 (cytotoxic T-lymphocyte antigen-4), PD-1 (programed death-1), Tim-3 (T cell immunoglobulin- and mucin domain-containing molecule 3), and TIGIT (T cell immunoreceptor with immunoglobulin and ITIM domains). While all of these coinhibitors share the T cell inhibitory capacity, each must be somewhat disparate in function since their respective deficiencies or dysfunctions are associated with different autoimmune states.

We discovered new coinhibitors in DC-HIL on APC and syndecan-4 (SD-4) on activated (but not resting) T cells (5, 6). DC-HIL belongs to the Ig receptor superfamily (95-120 KDa) expressed constitutively by epidermal Langerhans cells, DC, macrophages and other monocytes (7). Binding of DC-HIL to SD-4^{+} T cells strongly inhibits T cell activation triggered via the T cell receptor (TCR) (5, 7). Blocking such binding through soluble DC-HIL receptor or anti-SD-4 Ab augments delayed-type hypersensitivity responses (6, 8), and infusion of SD-$4^{-/-}$ T cells into sublethally γ-irradiated allogeneic mice worsened acute graft-versus-host disease (9).

We examined the role of the DC-HIL/SD-4 pathway in the activation of autoreactive T cells in experimental autoimmune encephalomyelitis (EAE), an animal model of multiple sclerosis (10). EAE immunization induced expression of SD-4 and DC-HIL on T cells and myeloid cells, respectively. Genetic deficiency of SD-4 or DC-HIL was associated with an hyperacute EAE phenotype, and adoptive transfer studies showed SD-$4^{-/-}$ T cells to be responsible for this disease exacerbation. Among DC-HIL^{+} myeloid cells in EAE-affected mice, $CD11b^{+}Gr1^{+}$ MDSC were the most expanded and most potent suppressors of T cell activation, and DC-HIL was proved to be the critical mediator of MDSC's suppressor function.

Materials and Methods

Mice

Female 6-8 wks-old C57BL/6 and $Rag2^{-/-}$ mice (B6(Cg)-*Rag2*$^{tm1.1Cgn}$/J) (11) were purchased from Harland Breeders (Indianapolis, IN) and Taconic Farms (Hudson, NY), respectively. SD-$4^{-/-}$ mice were produced by mating SD-$4^{+/-}$ mice (C57BL/6 genetic background) (12). DC-$HIL^{-/-}$mice were generated from embryonic stem cells derived from C57BL/6 mice backcrossed to C57BL/6 mice for 7 generations (manuscript submitted). Controls included DC-$HIL^{+/+}$ or SD-$4^{+/+}$ wild type (WT) from the same backcrossed generation. Following National Institutes of Health guidelines, mice were housed and cared for in a pathogen-free facility and subjected to experimental procedures approved by the Institutional Animal Care Use Center at UT Southwestern Medical Center.

Ab and immunofluorescent staining

mAb against CD3 (145-2C11), CD4 (RM4-5), CD8 (53-6.7), CD11b (M1/70), CD11c (N418), CD19 (eBio 1D3), CD28 (37,51), F4/80 (BM8), Gr-1 (RB6-8C5) and PD-1 (J43) were purchased from eBioscience (San Diego, CA); mAb against SD-4 (KY/8.2) from BD Pharmingen; and secondary Ab from Jackson ImmunoResearch. We generated UTX103 rabbit anti-DC-HIL mAb (13).

Single-cell suspensions from spleen or peripheral LNs were assayed for viability using trypan blue exclusion. When viability was <80%, live cells were enriched by Ficoll-gradient centrifugation for 20 min at room temperature (~90% for typical recovery). The cell suspension (5-10 × 10^{5}) was treated with 5 μg/ml Fc blocker (BD Pharmingen) on ice for 30 min and incubated with primary Ab (5-10 μg/ml), followed by addition of secondary Ab

(2.5 μg/ml). After washing, cell-bound fluorescence was analyzed by FACSCablibur (BD Biosciences) with a minimum of 10,000 events collected. Dead cells were excluded using 1 μg/ml propidium iodide.

Cell isolation

T cells, DC, macrophages, or MDSC were isolated from spleen of untreated or EAE-immunized WT or KO mice. $CD3^+$ T cells, DC, and macrophages were isolated using Pan-T cell isolation kit, anti-CD11c Ab-microbeads, and anti-F4/80 Ab-mirobeads (all from Miltenyi Biotec), respectively. For MDSC isolation, spleen cells were depleted of $CD19^+$, $CD11c^+$, $F4/80^+$ cells using beads conjugated with the corresponding Ab, and then positively purified using anti-CD11b-microbeads. Purity of all cell preparations was ~95%, as determined by flow cytometry. For depletion of DC-HIL^+ MDSC, spleen cells left after the first depletion were further depleted using biotin-binder beads (Invitrogen) precoated with anti-DC-HIL mAb or control IgG. $CD11b^+$ cells were purified as before, with former and latter fractions termed DC-HIL-depleted and undepleted MDSC, respectively. The DC-HIL-depleted preparation contained only a trace number (1-3%) of DC-HIL^+ cells. For isolation of central nervous system (CNS)-infiltrating cells, EAE-sick mice (14 days post-immunization) were perfused through the left cardiac ventricle with cold PBS. Their spinal cords were cut into small pieces and digested in 2.5 mg/ml Collagenase D (Roche)/1 mg/ml DNAse I (Sigma-Alrich) in DMEM at 37°C for 45 min. Cells were then suspend in 70 % percoll and overlaid with 37 % percoll. After centrifugation at 500 × g for 20 min., the interface between 2 layers was collected, spun down, and washed.

T cell suppression assays

T cells purified from spleen of naive mice were labeled with 1 μM carboxy-fluorescein diacetate succinimidyl ester (CFSE, Molecular Probes) in DPBS at 37°C for 15 min. After 30 min of incubation in culture media, labeled T cells were seeded in ELISA wells (2×10^5 cells/well) precoated with anti-CD3 and anti-CD28 Ab (each 1 μg/ml). To this culture, myeloid cells (MDSC, DC, or macrophages) purified from spleen of WT or KO mice (on day 10 post-EAE-immunization) were added at varying cell ratios. For inhibition studies, varying doses of anti-DC-HIL mAb, anti-cytokine Ab, control IgG, chemical inhibitors, catalase, or superoxide dismutase were added separately to cocultures of T cells (or spleen cells) and myeloid cells or MDSC (1:1 cell ratio). After culturing for 3 d, cells were harvested and examined for asynchronous cell division of CFSE fluorescence intensity using flow cytometry. The culture supernatant was recovered and assayed for IL-2 production by ELISA (eBioscience).

EAE and adoptive transfer

On day 0, mice were injected *s.c.* with 200 μg MOG peptide (MEVGWYRSPFSRVVHLYRNGK) in complete Freund's adjuvant (DIFCO Laboratories) containing heat-killed *Mycobacterium tuberculosis* H37 RA (500 μg). On days 0 and 2, mice were injected *i.p.* with 200 ng pertussis toxin (DIFCO Laboratories) (10). Disease was assessed in an unbiased manner and scored using an established scale (10). To assess MOG-specific T cell response in EAE-induced mice, spleen cells were prepared from mice immunized 10 d prior and seeded onto ELISPOT wells at varying cell densities in the presence of MOG peptide (5 μg/ml) for 2 d. IFN-γ- or IL-17-producing cells were counted using ELISPOT assay (eBiosciences).

For adoptive T cell transfer experiments, 1×10^7 T cells isolated from spleens of naive WT or SD-4 KO mice were injected *i.v.* into $Rag2^{-/-}$ mice (n=10). Next day, all mice were immunized with MOG peptide/adjuvant, followed by toxin injections. Mice were examined daily for signs of disease. To assess effects of DC-HIL^+ MDSC on EAE, MDSC were

isolated from pooled spleens of EAE-sick WT mice (10 mice on day 14 after EAE immunization), depleted or undepleted of DC-HIL$^+$ cells, and then injected *i.v.* into DC-HIL KO mice (5×10^6 cells/mouse) (n=10) that were EAE-immunized 4 d prior.

Activation of DC-HIL and soluble factors

MDSC (5×10^6) isolated from day 14 post-immunization were cultured in 96 well-plates (2×10^5 cells/well) precoated with anti-DC-HIL mAb or control IgG (10 μg/ml). After 1 or 2 d of culture, the culture supernatant and cell pellets were collected separately: the former tested for cytokine secretion using ELISA; and the latter assayed whole cell extracts for NO production using the Griess method (14). MDSC were also mixed with spleen cells (2×10^5 cells/well) from naive WT mice at increasing cell ratios and cultured for 2 d in wells precoated with anti-CD3/CD28 Ab (each 1 μg/ml). Cells were polled from 6 same wells and used for NO assay.

Histological examination

Twenty days after EAE-immunization, spinal cords were dissected from 3-4 representative mice in each group. Specimens were fixed in 4% neutral buffered formalin for 48 h, paraffin-embedded, thin-sectioned (6 μm), and stained with hematoxylin and eosin (H&E) according to Ehrlich (Sigma-Aldrich). Histological examination was carried out using Olympus BH2 microscope (Olympus) under 4X magnification.

Statistical analysis

Data are presented as means ± sd. Significant differences between experimental variables were determined using two-tailed Student's *t*-test, with $p<0.05$ considered significant. Statistical analysis of EAE clinical scores was performed by two-way analysis of variance (ANOVA). All data shown are representative of at least 2 independent experiments.

Results

EAE immunization induced T cells to express SD-4

Since negative regulators of T cell function restrict development of EAE (2), we posited the DC-HIL/SD-4 pathway to be involved. We first examined expression of SD-4 by T cells in spleen and draining lymph nodes (DLN) before and after EAE immunization, in comparison to expression of another T cell inhibitor, PD-1 (Fig. 1, A and B). Prior to immunization, there were very few SD-4-expressing T cells in either tissue, whereas PD-1$^+$ T cells were noted in greater numbers. After immunization, expression of both SD-4 and PD-1 rose among CD4$^+$ and CD8$^+$ cells, with varying kinetics that peaked on day 6, but declined slowly for spleen CD4$^+$ and CD8$^+$ and DLN CD4$^+$ cells (Fig. 1, A and B). By contrast, SD-4 expression continued to rise among DLN CD8$^+$ cells despite PD-1 expression falling to a lower level (Fig. 1B). Thus EAE immunization induced expression of SD-4 and PD-1 on T cells, with different kinetics in CD4$^+$ vs. CD8$^+$ cells, particularly in DLN.

Among DC-HIL-expressing myeloid cells in spleen during induction of EAE, MDSC are the most expanded population

We next examined frequencies of 3 types of myeloid cells in spleen (macrophages, DC, and MDSC) at different time points during EAE induction (Fig. 1C). Pre-immunization, all 3 cell types were present at very low frequencies (1-2%). Fourteen days after inducing EAE, those frequencies rose progressively (up to 10-40 %), with MDSC as the most expanded population (40%). DC-HIL was expressed by 50% of each cell type (Fig. 1D). We also examined DC-HIL and SD-4 expression by MDSC and T cells, respectively, isolated from the CNS of EAE-sick mice (14 days post-immunization). Of the CNS-infiltrating cells, 38%

of MDSC (representing at 30% among the total cells) expressed DC-HIL, and 44 to 47% of $CD4^+$ or $CD8^+$ T cells (minuscule fractions) expressed SD-4 (Fig. 1E). Thus, akin to expression of its ligand SD-4 on T cells, DC-HIL on myeloid cells was upregulated during EAE induction.

SD-4 inhibited EAE by negatively regulating autoreactive T cells

We next examined the functional significance of upregulated SD-4 expression on T cells during EAE induction in WT vs. SD-4 KO mice immunized with MOG peptide. From 5 to 13 days post-immunization, tails of WT mice remained flaccid (median score of 1.75 on day 10), but worsened to a peak score of 2.0 on day 20, that then regressed to 1.75 by day 30 (Fig. 2A). By contrast, SD-4 KO mice developed perceptibly hardened tails as early as days 4 to 7, but with an insignificantly higher score of 3.0 on day 10 ($p<0.1$) (Fig. 2B), worsening to 3.75 on day 30 ($p<0.001$) (Fig. 2C). Histologically, the spinal cord 20 days post-immunization (Fig. 2D) showed a more intense infiltrate in KO mice (clinical score of 4) vs. WT mice (score of 2). Finally, T cell activation was measured by the number of effector T cells: KO mice had markedly greater numbers of IFN-γ- or IL-17-secreting splenocytes 10 days after immunization (Fig. 2E). Thus SD-4 gene deletion augmented EAE severity associated with significantly more autoreactive T cells.

SD-4 deletion made T cells more potent inducers of EAE disease

Since SD-4 is also expressed by cells other than T cells (e.g., fibroblasts), we questioned whether increased susceptibility of SD-4 KO mice to EAE was due to greater responsiveness of SD-$4^{-/-}$ T cells. We isolated T cells from naive WT or SD-4 KO mice and adoptively transferred these cells into $Rag2^{-/-}$ mice that lack mature T cells (11). Control $Rag2^{-/-}$ mice without T cells (infused only with PBS) developed minimal EAE (score of 1.5) on days 15 to 25 (Fig. 3A). $Rag2^{-/-}$ mice injected with SD-$4^{+/+}$ T cells displayed similarly low disease severity that lasted longer, till day 40 (Fig. 3B). By contrast, injection of SD-$4^{-/-}$ T cells enhanced EAE (score of 4.5) on days 18 to 25 (Fig. 3C). Severity of EAE was tracked through early (day 10), mid (day 20), and later (day 30) phases (Fig. 3D). Injected SD-$4^{+/+}$ T cells worsened EAE only minimally during all 3 phases, especially since their changes were not statically significant compared to those in control $Rag2^{-/-}$ mice ($p>0.104$). By contrast, injected SD-$4^{-/-}$ T cells markedly exacerbated EAE during all phases. Moreover, histology of spiral cords from these mice showed significantly more infiltrating lymphocytes compared to those of $Rag2^{-/-}$ mice infused with SD-$4^{+/+}$ T cells (Fig. 3E). These differences ran parallel to increased numbers of IFN-γ and/or IL-17-producing effector T cells in spleen of EAE-induced SD-4 KO mice. Frequencies of Treg and memory T cells in the T cell preparation used for this adoptive transfer were similar between WT and KO mice (data not shown). Thus SD-4 gene deletion augmented reactivity of T cells to MOG.

DC-HIL deletion increased susceptibility to EAE

Because DC-HIL expression rose in EAE-induced mice, we inferred that DC-HIL suppresses induction of EAE. To confirm this postulate, we compared EAE induction in WT vs. DC-HIL KO mice. Note that KO mice did not exhibit any gross abnormality or developmental defect of lymphoid organs (manuscript submitted). WT mice manifested EAE 5 to 12 days after immunization, reaching a peak score of 3.0 on days 10 to 30 (Fig. 4A). Like SD-4 KO mice, DC-HIL KO mice also manifested EAE by days 3 to 5, peaking on days 12 to 25, with the disease lasting through day 40 (Fig. 4B). Average scores for DC-HIL KO mice were markedly greater than for WT mice in all phases of EAE induction ($p<0.01$) (Fig. 4C). KO mice's spinal cords had greater numbers of infiltrating lymphocytes (Fig. 4D), and ELISPOT assays revealed markedly more effector T cells in their spleens (Fig. 4E). Thus DC-HIL deletion worsened EAE.

DC-HIL-expressing MDSC are potent suppressors of T cell function in EAE

Theorizing that DC-HIL-expressing myeloid cells are the most potent T cell suppressors in EAE-afflicted mice, we purified F4/80$^+$ macrophages, CD11c$^+$ DC, or CD11b$^+$Gr-1$^+$ MDSC from splenocytes of WT mice 10 days after MOG immunization. Each cell type was assayed for T cell-suppressor activity, in which increasing cell numbers were added to CFSE-labeled T cells activated by anti-CD3/CD28 Ab (Fig. 5A). T cell activation was measured by CFSE dilution assays. Neither macrophages nor DC from EAE-sick mice inhibited T cell activation, whereas MDSC caused suppression in a dose-dependent manner. We next addressed whether DC-HIL was responsible for MDSC-suppressor function by assaying the T cell-inhibitory activity of MDSC (vs. other myeloid cells) purified from EAE-affected DC-HIL KO mice (Fig. 5B). DC-HIL deletion had no effect on the suppressor activity of macrophages or DC, but it markedly reduced MDSC suppressor function (T cell proliferation rose from 26% to 83% at the highest ratio). Results of IL-2 secretion assays were consistent with the proliferation assays (Fig. 5C). We further examined DC-HIL's critical role in MDSC suppressor function (Fig. 6) by adding anti-DC-HIL mAb (but not control IgG) to T cell/MDSC cocultures: inclusion of the anti-DC-HIL mAb restored MSDC-inhibited T cell activation in a dose-dependent fashion as measured by CFSE-proliferation assays (Fig. 6A). The same mAb had only minuscule effect on macrophages or DC. Similar results were obtained by IL-2 production assays (Fig. 6B). These outcomes indicate that deletion of the DC-HIL gene or inhibition of DC-HIL activity leads to functionally defective MDSC that may be responsible for increased severity of EAE.

Activation of DC-HIL induced MDSC expression of INF-γ, nitric oxide (NO), and reactive oxygen species (ROS)

Since T cell-inhibitory soluble factors are critical mediators for MDSC function, including cytokines, urea/L-ornithine produced by arginase I (15), NO (16), and ROS (17), we examined their influence on MDSC' suppressor activity by adding specific inhibitors to cocultures of spleen cells and MDSC isolated from EAE-affected mice. Whereas Ab neutralizing IL-10 or TGF-β1 had no effect on suppressor activity, anti-IFN-γ Ab abrogated it completely (Fig. 7A). Inhibitors for ariginase I, indoleamine, or ROS had little-to-no effect, but inhibitors of NO synthases or iNOS respectively blocked suppression substantially or completely (Fig. 7B). We then addressed association of DC-HIL with expression of these soluble factors. MDSC were cultured with immobilized anti-DC-HIL mAb (to activate DC-HIL receptor) and examined for expression of IFN-γ, NO, and ROS. Anti-DC-HIL treatment induced MDSC expression of IFN-γ 40-fold greater than control IgG-treatment; and TNF-β was also upregulated (10-fold); but there was no significant effect on IL-10 and TGF-β expression (Fig. 7C). Ab treatment also increased MDSC expression of ROS and NO, compared to controls (Fig. 7 D and E). Both IFN-γ and NO expression were enhanced, highest on day 1, followed by a quick fall on the next day. We then addressed whether DC-HIL is critically involved in NO production by MDSC during coculturing with T cells. MDSC isolated from EAE-affected WT or DC-HIL KO mice were added to culture of spleen cells from WT mice activated by anti-CD3/CD28 Ab, and NO production measured (Fig. 7F). Addition of WT-MDSC increased markedly NO production compared to spleen cells alone, whereas DC-HIL$^{-/-}$ MDSC failed to produce NO. Altogether, IFN-γ and NO were critical mediators of the suppressor activity of MDSC induced in EAE-affected mice, the expression of which was induced at least through activation of DC-HIL.

DC-HIL$^+$ MDSC from EAE-affected WT mice reduced disease severity in DC-HIL KO mice

To determine whether DC-HIL$^+$ MDSC are responsible for exacerbated EAE in DC-HIL KO mice, we purified MDSC from spleens of WT mice immunized 10 days prior for EAE. These cells were depleted (or undepleted) of DC-HIL$^+$ cells and then infused into DC-HIL KO mice 4 days after EAE immunization (Fig. 8). Control mice (WT and DC-HIL KO mice

injected with PBS) were also immunized in parallel and scored clinically. WT and KO mice developed EAE similar to previous experiments (Fig. 8, A and B). Injection of undepleted MDSC (containing 50% DC-HIL$^+$ cells) into DC-HIL KO mice reduced disease severity compared to PBS-treated DC-HIL KO mice (2.5 median score vs. 4.0, $p<0.01$) as assessed on day 10, though both disease scores were higher than for EAE-treated WT mice (2.0) (Fig. 8C). However, score differences between MDSC-injected KO and PBS-injected WT mice became smaller and eventually insignificant in later phases (2.5 vs. 4.5 on day 20 with $p=0.6$, and 4.0 vs. 3.0 on day 30 with $p=0.06$) (Fig. 8E). By contrast, DC-HIL KO mice injected with DC-HIL-depleted MDSC developed EAE as severely as those treated with PBS alone (Fig. 8D). These outcomes were associated with markedly increased numbers of IFN-γ/IL-17-producing effector T cells (Fig. 8F). Thus infusion of DC-HIL$^+$ MDSC alleviated EAE exacerbated by DC-HIL deletion, indicating that increased severity of EAE in DC-HIL KO mice was due to functionally defective MDSC.

Discussion

Activation of autoreactive T cells by autoantigen-loaded APC triggers competing costimulatory and coinhibitory linkages that determine whether the net TCR signaling is immunostimulatory or tolerogenic. Our findings indicate that the DC-HIL/SD-4 pathway is an important down-regulator of autoimmune responses since genetic deficiency of either DC-HIL or SD-4 increased host susceptibility to EAE and this hyperacute phenotype could be transferred to Rag2$^{-/-}$ mice by infusion of SD-4^{neg} T cells during immunization for EAE. Moreover, infusion of DC-HIL$^+$ (but not DC-HIL^{neg}) MDSC from EAE-affected WT mice into DC-HIL KO mice with EAE alleviated the autoimmune disease's severity.

How does the DC-HIL/SD-4 pathway compare with other coinhibitory systems? CTLA-4, expressed constitutively and exclusively by T cells, is key to maintaining central and peripheral tolerance, which it implements via Tregs (15,16). CTLA KO mice spontaneously develop lethal autoimmune disease involving multiple organs (18). PD-1 also regulates central and peripheral tolerance, and like CTLA-4 it does so via Tregs (19). Unlike CTLA-4, PD-1 is expressed by a wider range of cells including T and B cells, natural killer (NK) T cells, DC, other monocytes, and thymocytes (20). PD-1 KO mice spontaneously develop a lupus erythematosus-like disease, but at a later age than CTLA-4 KO mice and with milder forms of glomerulonephritis or cardiomyopathy (21). TIGIT has a similar cell expression profile as PD-1 and resembles CTLA-4 in its ability to bind the competing ligands CD155 and CD112 expressed by APC and non-lymphoid cells (22, 23). While TIGIT KO mice do not spontaneously develop autoimmune disease, these animals manifest EAE spontaneously when crossed with $MOG_{35–55}$-specific TCR transgenic 2D2 mice (23). Finally, Tim-3 is expressed by CD4$^+$ Th1, but not Th2 cells (24) and its functional blockade causes hyperacute EAE in mice (25).

SD-4 differs from the aforementioned coinhibitors by its restricted expression to only some effector/memory T cells and by absence of direct physical interaction with the TCR. Instead SD-4, which lacks an intracellular immunoreceptor tyrosine-based inhibitory motif (21), suppresses T cell activation by stimulating CD148 via its protein tyrosine phosphatase activity (26). Most importantly, SD-4's suppressor function is independent of Treg function. Indeed, SD-4 has never been shown to be expressed by Tregs *in vivo*, although it has been induced on these cells following *in vitro* stimulation by anti-CD3 Ab (9). DC-HIL also differs from other coinhibitory ligands by its expression on non-lymphoid cells (melanocytes, keratinocytes, and osteoblasts) and by having an intracellular immunoreceptor tyrosine-based activation motif (ITAM) (27-29). Having shown previously that crosslinking of DC-HIL receptor with specific Ab induced tyrosine phosphorylation of the ITAM (13), we hypothesized that DC-HIL activation induces MDSC to express IFN-γ, NO, and ROS via

these ITAM-linked signal pathways. We are currently studying the DC-HIL-induced signal pathway in MDSC.

MDSC are potent inhibitors of T cell function; their expansion in blood and tissues has been associated with cancer growth (27) and chronic inflammatory conditions including bacterial and parasitic infections as well as autoimmune diseases (28). In particular, $CD11b^{+}Gr\text{-}1^{+}$ MDSC (including $CD11b^{+}Ly6C^{+}$ cells) have been isolated from autoimmune inflammatory environments (30). While their potent immunosuppressive function is beyond dispute, it is not clear whether they are pathologic or protective for autoimmune diseases. A pathologic role for MDSC in EAE has been supported by studies showing that: (1) blood $CD11b^{+}Ly6C^{high}$ cells migrated into the CNS to become inflammatory APC that activate autoreactive T cells (30, 31); and (2) anti-Gr-1 Ab-mediated depletion of $CD11b^{+}Gr\text{-}1^{+}$MDSC reduced severity of EAE induced by Theiler's murine encephalomyelitis virus (TMEV) infection in mice (32). By contrast, a protective role for MDSC has been buttressed by the following findings: (1) blood MDSC in naive mice were potent T cell suppressors and their loss of function promoted EAE (33); and (2) MDSC reduced inflammation in the central nerve system by promoting T cell apoptosis (34).

Our findings favor a protective role for MDSC in EAE since $CD11b^{+}Gr\text{-}1^{+}$ MDSC containing a subset expressing DC-HIL strongly suppressed T cell function and adoptive transfer of DC-HIL^{+} MDSC (from EAE-affected mice) alleviated the hyperacute EAE phenotype in DC-HIL KO mice. These outcomes are consistent with those from mouse models of inflammatory bowel disease (35), alopecia areata (36), and type 1 diabetes (37). The seemingly contradictory roles for MDSC in autoimmunity may be due to divergent genetic backgrounds of mouse strains used, that in turn leads to disparate responses to autoantigens by different MDSC subsets (38).

Mice lacking DC-HIL/SD-4 pathway appear to develop large expansion of the pathogenic T cells in peripheral tissues during induction of EAE. Similar expansion was noted in spleen of DC-$HIL^{-/-}$ or SD-$4^{-/-}$ mice following allogeneic BM transplantation (B57BL/6 BM cells injected into total body γ-irradiated BLAB/c mice) (9) and contact hypersensitivity induced by the chemical allergen oxazolone (unpublished data). This expansion may be caused by synergistic effects of hyper-active APC and disabled MDSC lacking the DC-HIL pathway: In EAE-sick mice, we speculate that T cells may be hyper-activated by DC-$HIL^{-/-}$ APC because these cells possessed 2-fold greater T cell-stimulatory capacity than WT counterparts (manuscript submitted). Moreover, their activation may not be suppressed efficiently by DC-$HIL^{-/-}$ MDSC, suppressors most expanded and most potent in EAE-sick mice. Because MDSC migrate into inflamed tissues and other organs (e.g., spleen, LN, and kidney), T cells could be hyper-activated in many organs, particularly in regional LN where inflammatory APC accumulated.

Tolerogenic DC generated from *ex vivo* culture have been used to vaccinate against autoimmune diseases (39). Such DC can expand Tregs and render autoreactive T cells anergic in an Ag-specific manner (39). MDSC may possibly be exploited in a similar manner (40) with potentially greater potency as protectors against autoimmunity, given their added ability to inhibit NK-cell activity (41) and macrophage cytokine production (42), and in an Ag-non-specific way.

In summary, in the DC-HIL/SD-4 pathway, we have uncovered a new negative regulator of autoimmune responses that works via MDSC-mediated T cell suppression. Because MDSC are distinct targets from those of other coinhibitory pathways and because DC-HIL induces expression of T cell-inhibitory factors required for MDSC's suppressor activity, the DC-

HIL/SD-4 pathway represents an opportune platform for studying autoimmune regulation and a promising focus for treatment of autoimmune disease.

Acknowledgments

We thank Irene Dougherty and Megan Randolph for technical and secretary assistance.

This research was supported by the National Institutes of Health grant (AI064927-05). Correspondence address: Dr. Kiyoshi Ariizumi, Department of Dermatology, The University of Texas Southwestern Medical Center, 5323 Harry Hines Blvd, Dallas TX 75390-9069.

Abbreviations used in this article

DC	Dendritic cells
DC-HIL	DC-associated heparan sulfate proteoglycan-dependent integrin ligand
EAE	Experimental autoimmune encephalomyelitis
iNOS	Inducible nitric oxide synthase
ITAM	Immunoreceptor tyrosine-based activation motif
KO	Knocked out
LN	Lymph node
MDSC	Myeloid-derived suppressor cells
NO	Nitric oxide
PD-1	Programed death-1
ROS	Reactive oxygen species
SD-4	Syndecan-4
TIGIT	T cell immunoreceptor with immunoglobulin and ITIM domains
Tim-3	T cell immunoglobulin- and mucin domain-containing molecule 3
Treg	Regulatory T cells
WT	Wild type

References

1. Lohmann T, Leslie RD, Londei M. T cell clones to epitopes of glutamic acid decarboxylase 65 raised from normal subjects and patients with insulin-dependent diabetes. J Autoimmun. 1996; 9:385–389. [PubMed: 8816975]
2. Joller N, Peters A, Anderson AC, Kuchroo VK. Immune checkpoints in central nervous system autoimmunity. Immunol Rev. 2012; 248:122–139. [PubMed: 22725958]
3. Cripps JG, Gorham JD. MDSC in autoimmunity. Int Immunopharmacol. 2011; 11:789–793. [PubMed: 21310255]
4. Serafini P, Mgebroff S, Noonan K, Borrello I. Myeloid-derived suppressor cells promote cross-tolerance in B-cell lymphoma by expanding regulatory T cells. Cancer Res. 2008; 68:5439–5449. [PubMed: 18593947]
5. Chung JS, Sato K, Dougherty II, Cruz PD Jr. Ariizumi K. DC-HIL is a negative regulator of T lymphocyte activation. Blood. 2007; 109:4320–4327. [PubMed: 17284525]
6. Chung JS, Dougherty I, Cruz PD Jr. Ariizumi K. Syndecan-4 mediates the coinhibitory function of DC-HIL on T cell activation. J Immunol. 2007; 179:5778–5784. [PubMed: 17947650]

7. Chung JS, Bonkobara M, Tomihari M, Cruz PD Jr. Ariizumi K. The DC-HIL/syndecan-4 pathway inhibits human allogeneic T-cell responses. Eur J Immunol. 2009; 39:965–974. [PubMed: 19350579]

8. Akiyoshi H, Chung JS, Tomihari M, Cruz PD Jr. Ariizumi K. Depleting syndecan-4+ T lymphocytes using toxin-bearing dendritic cell-associated heparan sulfate proteoglycan-dependent integrin ligand: a new opportunity for treating activated T cell-driven disease. J Immunol. 2010; 184:3554–3561. [PubMed: 20176742]

9. Chung JS, Tomihari M, Tamura K, Kojima T, Cruz PD Jr. Ariizumi K. The DC-HIL ligand syndecan-4 is a negative regulator of T-cell allo-reactivity responsible for graft-versus-host disease. Immunology. 2013; 138:173–182. [PubMed: 23113638]

10. Stromnes IM, Goverman JM. Active induction of experimental allergic encephalomyelitis. Nat Protoc. 2006; 1:1810–1819. [PubMed: 17487163]

11. Hao Z, Rajewsky K. Homeostasis of peripheral B cells in the absence of B cell influx from the bone marrow. J Exp Med. 2001; 194:1151–1164. [PubMed: 11602643]

12. Ishiguro K, Kadomatsu K, Kojima T, Muramatsu H, Tsuzuki S, Nakamura E, Kusugami K, Saito H, Muramatsu T. Syndecan-4 deficiency impairs focal adhesion formation only under restricted conditions. J Biol Chem. 2000; 275:5249–5252. [PubMed: 10681494]

13. Chung JS, Yudate T, Tomihari M, Akiyoshi H, Cruz PD Jr. Ariizumi K. Binding of DC-HIL to dermatophytic fungi induces tyrosine phosphorylation and potentiates antigen presenting cell function. J Immunol. 2009; 183:5190–5198. [PubMed: 19794069]

14. De Santo C, Serafini P, Marigo I, Dolcetti L, Bolla M, Del Soldato P, Melani C, Guiducci C, Colombo MP, Iezzi M, Musiani P, Zanovello P, Bronte V. Nitroaspirin corrects immune dysfunction in tumor-bearing hosts and promotes tumor eradication by cancer vaccination. Proc Natl Acad Sci U S A. 2005; 102:4185–4190. [PubMed: 15753302]

15. Rodriguez PC, Ochoa AC. Arginine regulation by myeloid derived suppressor cells and tolerance in cancer: mechanisms and therapeutic perspectives. Immunol Rev. 2008; 222:180–191. [PubMed: 18364002]

16. Bingisser RM, Tilbrook PA, Holt PG, Kees UR. Macrophage-derived nitric oxide regulates T cell activation via reversible disruption of the Jak3/STAT5 signaling pathway. J Immunol. 1998; 160:5729–5734. [PubMed: 9637481]

17. Kusmartsev S, Gabrilovich DI. Inhibition of myeloid cell differentiation in cancer: the role of reactive oxygen species. J Leukoc Biol. 2003; 74:186–196. [PubMed: 12885935]

18. Waterhouse P, Penninger JM, Timms E, Wakeham A, Shahinian A, Lee KP, Thompson CB, Griesser H, Mak TW. Lymphoproliferative disorders with early lethality in mice deficient in Ctla-4. Science. 1995; 270:985–988. [PubMed: 7481803]

19. Francisco LM, Sage PT, Sharpe AH. The PD-1 pathway in tolerance and autoimmunity. Immunol Rev. 2010; 236:219–242. [PubMed: 20636820]

20. Nishimura H, Agata Y, Kawasaki A, Sato M, Imamura S, Minato N, Yagita H, Nakano T, Honjo T. Developmentally regulated expression of the PD-1 protein on the surface of double-negative (CD4-CD8-) thymocytes. Int Immunol. 1996; 8:773–780. [PubMed: 8671666]

21. Nishimura H, Nose M, Hiai H, Minato N, Honjo T. Development of lupus-like autoimmune diseases by disruption of the PD-1 gene encoding an ITIM motif-carrying immunoreceptor. Immunity. 1999; 11:141–151. [PubMed: 10485649]

22. Yu X, Harden K, Gonzalez LC, Francesco M, Chiang E, Irving B, Tom I, Ivelja S, Refino CJ, Clark H, Eaton D, Grogan JL. The surface protein TIGIT suppresses T cell activation by promoting the generation of mature immunoregulatory dendritic cells. Nat Immunol. 2009; 10:48–57. [PubMed: 19011627]

23. Joller NH, J. P. Brynedal B, Kassam N, Spoerl S, Levin SD, Sharpe AH, Kuchroo VK. Cutting edge: TIGIT has T cell-intrinsic inhibitory functions. J Immunol. 2011; 186:1338–1342. [PubMed: 21199897]

24. Sanchez-Fueyo A, Tian J, Picarella D, Domenig C, Zheng XX, Sabatos CA, Manlongat N, Bender O, Kamradt T, Kuchroo VK, Gutierrez-Ramos JC, Coyle AJ, Strom TB. Tim-3 inhibits T helper type 1-mediated auto- and alloimmune responses and promotes immunological tolerance. Nat Immunol. 2003; 4:1093–1101. [PubMed: 14556005]

25. Monney L, Sabatos CA, Gaglia JL, Ryu A, Waldner H, Chernova T, Manning S, Greenfield EA, Coyle AJ, Sobel RA, Freeman GJ, Kuchroo VK. Th1-specific cell surface protein Tim-3 regulates macrophage activation and severity of an autoimmune disease. Nature. 2002; 415:536–541. [PubMed: 11823861]
26. Chung JS, Cruz PD Jr. Ariizumi K. Inhibition of T-cell activation by syndecan-4 is mediated by CD148 through protein tyrosine phosphatase activity. Eur J Immunol. 2011; 41:1794–1799. [PubMed: 21469128]
27. Tomihari M, Hwang SH, Chung JS, Cruz PD Jr. Ariizumi K. Gpnmb is a melanosome-associated glycoprotein that contributes to melanocyte/keratinocyte adhesion in a RGD-dependent fashion. Exp Dermatol. 2009; 18:586–595. [PubMed: 19320736]
28. Safadi FF, Xu J, Smock SL, Rico MC, Owen TA, Popoff SN. Cloning and characterization of osteoactivin, a novel cDNA expressed in osteoblasts. J Cell Biochem. 2001; 84:12–26. [PubMed: 11746512]
29. Shikano S, Bonkobara M, Zukas PK, Ariizumi K. Molecular cloning of a dendritic cell-associated transmembrane protein, DC-HIL, that promotes RGD-dependent adhesion of endothelial cells through recognition of heparan sulfate proteoglycans. J Biol Chem. 2001; 276:8125–8134. [PubMed: 11114299]
30. Zhu B, Bando Y, Xiao S, Yang K, Anderson AC, Kuchroo VK, Khoury SJ. CD11b+Ly-6C(hi) suppressive monocytes in experimental autoimmune encephalomyelitis. J Immunol. 2007; 179:5228–5237. [PubMed: 17911608]
31. King IL, Dickendesher TL, Segal BM. Circulating Ly-6C+ myeloid precursors migrate to the CNS and play a pathogenic role during autoimmune demyelinating disease. Blood. 2009; 113:3190–3197. [PubMed: 19196868]
32. Bowen JL, Olson JK. Innate immune CD11b+Gr-1+ cells, suppressor cells, affect the immune response during Theiler's virus-induced demyelinating disease. J Immunol. 2009; 183:6971–6980. [PubMed: 19890055]
33. Slaney CY, Toker A, La Flamme A, Bäckström BT, Harper JL. Naïve blood monocytes suppress T-cell function. A possible mechanism for protection from autoimmunity. Immunol Cell Biol. 2011; 89:7–13. [PubMed: 21060323]
34. Moliné-Velázquez, V.; Cuervo, H.; Vila-Del Sol, V.; Ortega, MC.; Clemente, D.; de Castro, F. In Brain Pathol. 2011; Jun 9.. 2011 Myeloid-derived suppressor cells limit the inflammation by promoting T lymphocyte apoptosis in the spinal cord of a murine model of multiple sclerosis.; p. 678-691.
35. Westendorf AM, Fleissner D, Deppenmeier S, Gruber AD, Bruder D, Hansen W, Liblau R, Buer J. Autoimmune-mediated intestinal inflammation-impact and regulation of antigen-specific CD8+ T cells. Gastroenterology. 2006; 131:510–524. [PubMed: 16890605]
36. Marhaba R, Vitacolonna M, Hildebrand D, Baniyash M, Freyschmidt-Paul P, Zöller M. The importance of myeloid-derived suppressor cells in the regulation of autoimmune effector cells by a chronic contact eczema. J Immunol. 2007; 179:5071–5081. [PubMed: 17911592]
37. Yin B, Ma G, Yen CY, Zhou Z, Wang GX, Divino CM, Casares S, Chen SH, Yang WC, Pan PY. Myeloid-derived suppressor cells prevent type 1 diabetes in murine models. J Immunol. 2010; 185:5828–5834. [PubMed: 20956337]
38. Youn JI, Gabrilovich DI. The biology of myeloid-derived suppressor cells: the blessing and the curse of morphological and functional heterogeneity. Eur J Immunol. 2010; 40:2969–2975. [PubMed: 21061430]
39. Gross CC, Wiendl H. Dendritic cell vaccination in autoimmune disease. Curr Opin Rheumatol. 2013; 25:268–274. [PubMed: 23370378]
40. Zhou Z, French DL, Ma G, Eisenstein S, Chen Y, Divino CM, Keller G, Chen SH, Pan PY. Development and function of myeloid-derived suppressor cells generated from mouse embryonic and hematopoietic stem cells. Stem Cells. 2010; 28:620–632. [PubMed: 20073041]
41. Liu C, Yu S, Kappes J, Wang J, Grizzle WE, Zinn KR, Zhang HG. Expansion of spleen myeloid suppressor cells represses NK cell cytotoxicity in tumor-bearing host. Blood. 2007; 109:4336–4342. [PubMed: 17244679]

42. Sinha P, Clements VK, Bunt SK, Albelda SM, Ostrand-Rosenberg S. Cross-talk between myeloid-derived suppressor cells and macrophages subverts tumor immunity toward a type 2 response. J Immunol. 2007; 179:977–983. [PubMed: 17617589]

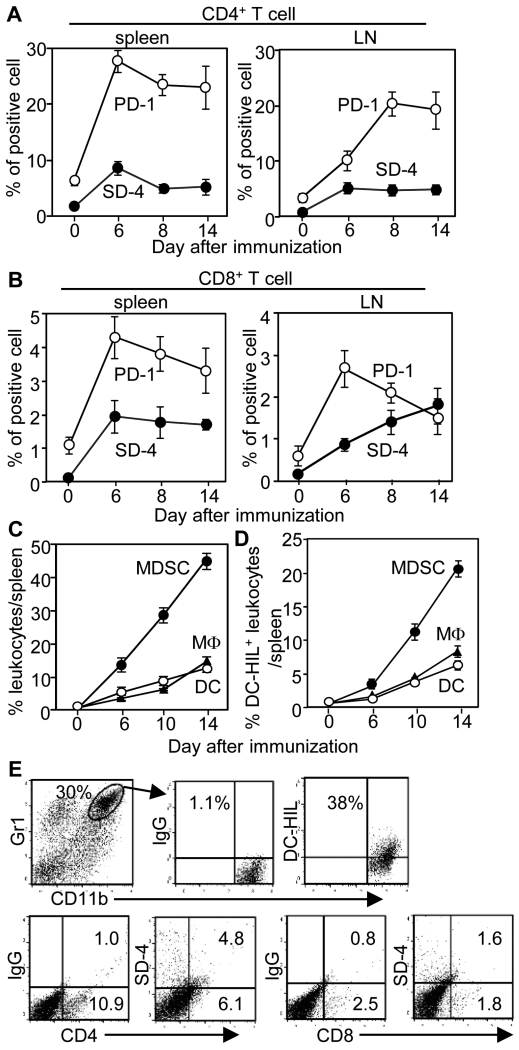

Figure 1. Kinetics of SD-4 or DC-HIL expression in T cells or myeloid cells during induction of EAE

Spleen or draining LN cells were prepared from WT mice at different time points (days) after EAE-immunization and examined by flow cytometry for frequency (%) of SD-4$^+$ or PD-1$^+$ cells in the total number of CD4$^+$ (**A**) or CD8$^+$ T cells (**B**). Data (mean ± sd, n=3) are plotted on time points. (**C** and **D**) Similar preparations from spleens were also examined for frequency of CD11b$^+$Gr-1$^+$ MDSC, F4/80$^+$ macrophages (MΦ), or CD11c$^+$ DC (**C**), and for proportion of DC-HIL$^+$ cells in each myeloid population (**D**). (**E**) Fourteen days post-EAE-immunization, CNS-infiltrating cells were isolated and assayed for frequency of CD11b$^+$Gr1$^+$ cells, CD4$^+$, and CD8$^+$ T cells, in which DC-HIL or SD-4 expression was measured. Data shown are representative of 3 independent experiments.

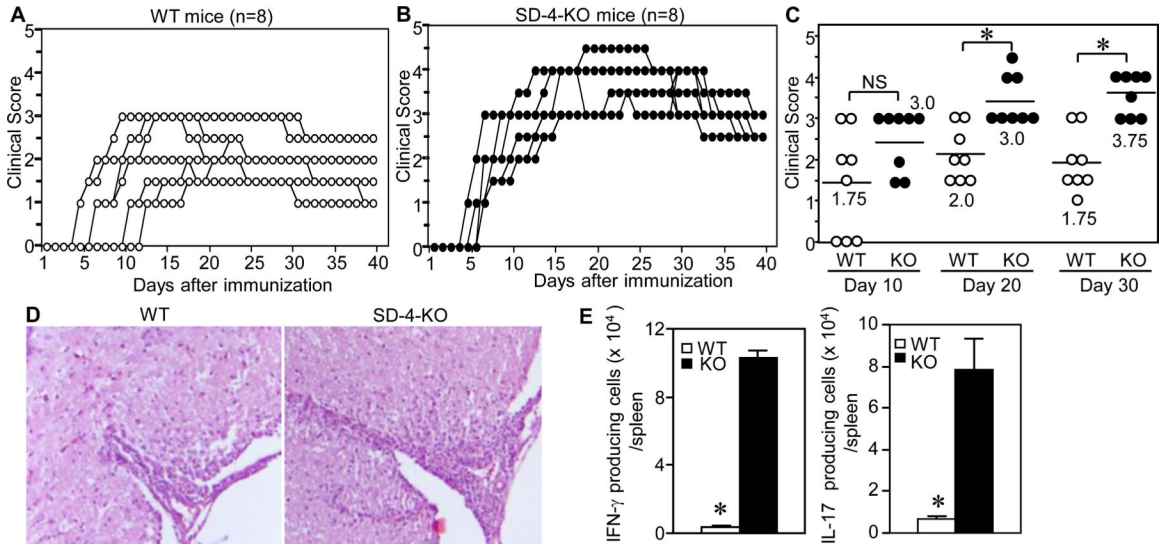

Figure 2. SD-4$^{-/-}$ mice develop significantly worse EAE

WT (**A**) or SD-4 KO (**B**) mice (n=8) were immunized with MOG peptide and complete Freund's adjuvant on day 0 and boosted with pertussis toxin on days 0 and 2. Kinetics of EAE development were monitored by clinical score of each mouse, plotted in a graphic version. Clinical score: 0, no abnormality; 1, flaccid tail; 2, moderate hind limb weakness; 3, severe hind limb weakness; 4, complete hind limb paralysis; and 5, quadriplegia, moribund state. (**C**) Clinical scores in early- (day 10), mid- (day 20) or late-phases (day 30) were plotted on a scatter chart (median, n=8), with statistical significance of scores (ANOVA, *p<0.001; NS, not significant) between WT and KO mice. (**D**) Spinal cords of mice 20 d after immunization were stained with H&E and examined under a microscope (4 X magnification). (**E**) IFN-γ- or IL-17-producing cells in spleen of WT and KO mice 10 d after immunization were enumerated by ELISPOT assay and calculated as number per spleen. *p<0.001 between WT and KO mice. All data shown are representative of 3 separate experiments.

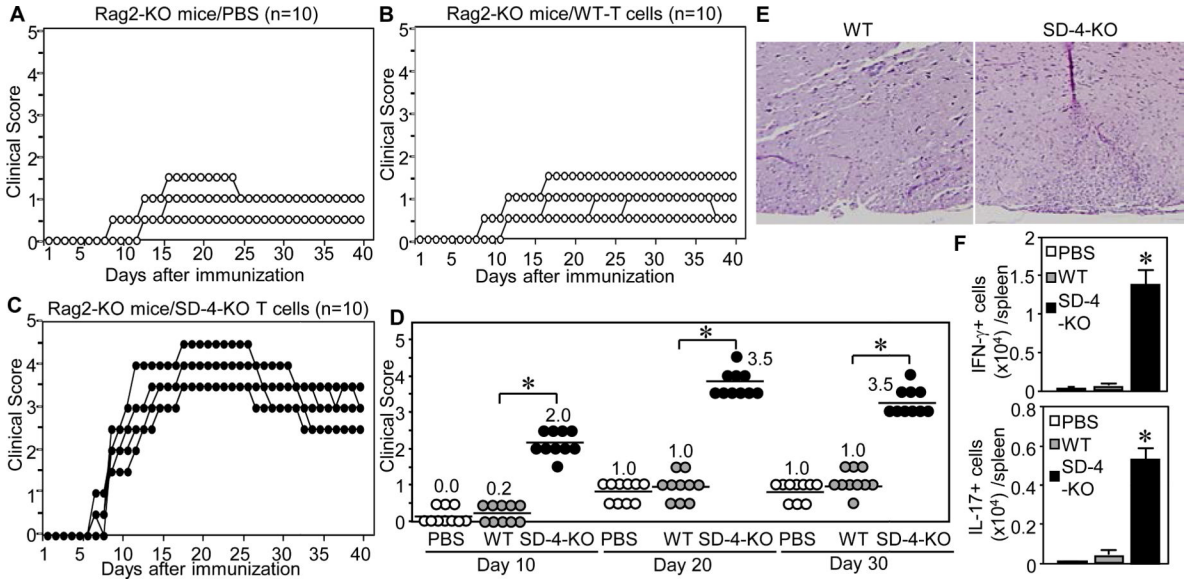

Figure 3. Adoptively transferred SD-4$^{-/-}$ T cells into Rag2$^{-/-}$ mice exacerbate EAE

Rag2$^{-/-}$mice (n=10) were injected *i.v.* with PBS alone (**A**), T cells isolated from naive WT (**B**) or SD-4 KO (**C**) mice, and EAE-immunized. Clinical scores (median) were assessed daily, plotted in a scatter chart, and sorted to early- (day 10), mid- (day 20) or late-phases (day 30) (**D**) with statistical significance of scores (*p<0.01) between mice injected with WT-T cells and KO-T cells. (**E**) Spinal cords of mice (injected with T cells from WT or KO mice) 20 days after immunization were stained with H&E and examined under a microscope (4 X magnification). (**F**) IFN-γ- or IL-17-producing cells from spleen of mice injected with PBS, or T cells from WT or KO mice 10 days after immunization were counted by ELISPOT assay and calculated as number per spleen. *p<0.001 between WT- and KO-T cells. Data are representative of 2 independent experiments.

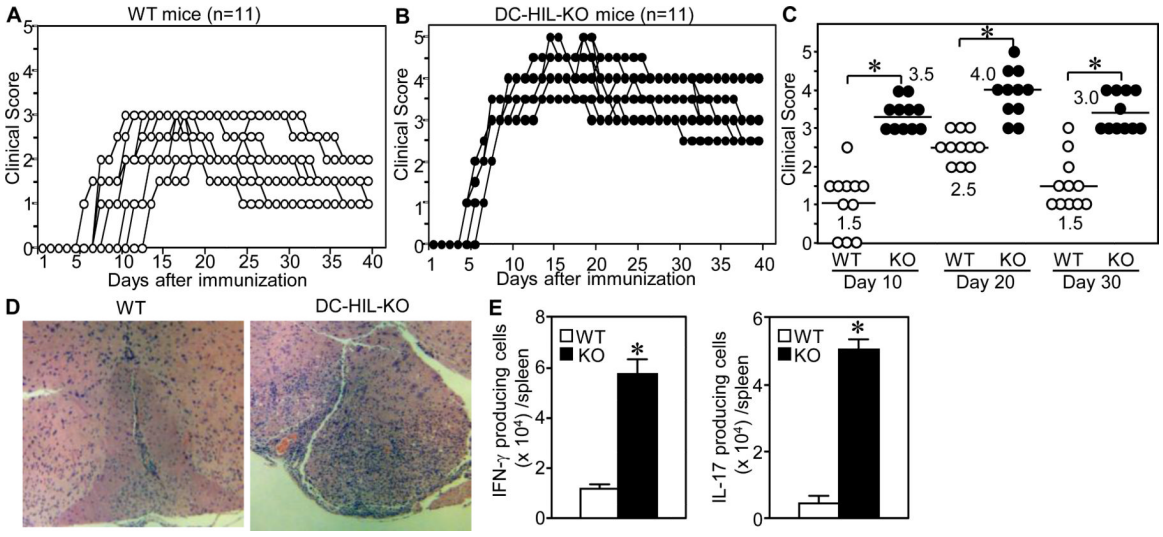

Figure 4. DC-HIL$^{-/-}$ mice developed hyperacute EAE after immunization with MOG peptide

WT (**A**) or DC-HIL KO (**B**) mice (n=11) were immunized similarly with MOG peptide and complete Freund's adjuvant, and EAE development monitored by scoring clinical symptoms. (**C**) Each clinical score on early- (day 10), mid- (day 20) or late-phases (day 30) was plotted in a scatter chart (median) with statistical significance of scores (*p<0.01) between WT and KO mice. Similarly, spinal cords of mice were examined histologically (**D**), and IFN-γ- or IL-17-producing cells from spleen of WT and KO mice counted and calculated (**E**). *p<0.0001 between WT and KO mice. Data are representative of 3 independent experiments.

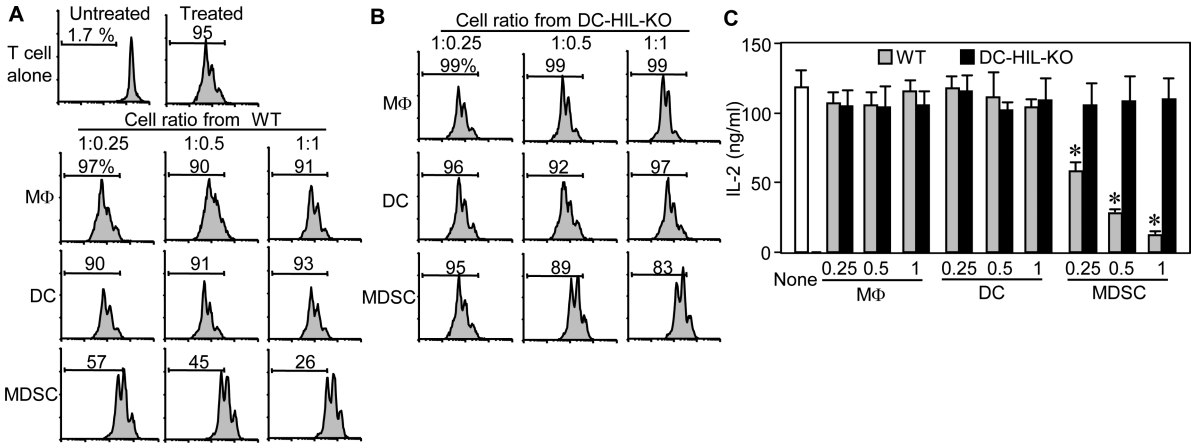

Figure 5. Among DC-HIL-expressing myeloid cells in EAE-developing mice, MDSC are the most potent suppressors

(**A** and **B**) Three myeloid cell subsets were purified from spleen of WT (**A**) or DC-HIL KO (**B**) mice that were EAE-immunized 10 days prior. These cells were assayed separately for T cell-suppressive activity by coculturing with CFSE-labeled WT-T cells at varying cell ratios in the presence of anti-CD3/CD28 Ab. Three days after culture, % of proliferated cells was examined by flow cytometry and data are shown in histograms. (**C**) Similar assays were performed, but with unlabeled T cells. T cell activation is shown by IL-2 production (mean ± sd, n=3). "None" means T cells and Ab without myeloid cells. *p<0.001 between WT and KO mice. Data are representative of 3 independent experiments.

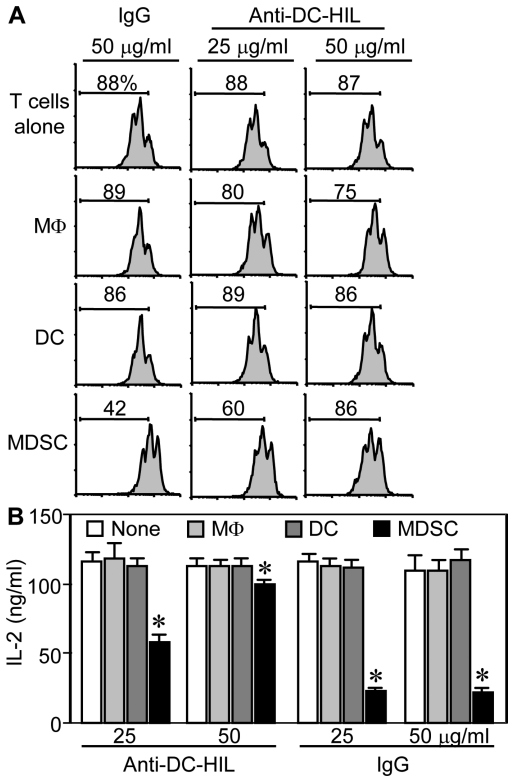

Figure 6. Anti-DC-HIL treatment abrogated T cell-suppressive activity of MDSC

Each myeloid cell subset was purified from EAE-disease mice and cocultured with CFSE-labeled WTT cells activated by anti-CD3/CD28 Ab in the presence of anti-DC-HIL mAb or control Ab (IgG) at 25 or 50 μg/ml. Dilution of CFSE fluorescent intensity was measured by flow cytometry (**A**) or IL-2 production assayed (**B**) (mean ± sd, n=3). "T cells alone" mean T cell culture with anti-CD3/CD28 cells but without myeloid cells. *p<0.001 between DC and MDSC. Data are representative of 3 independent experiments.

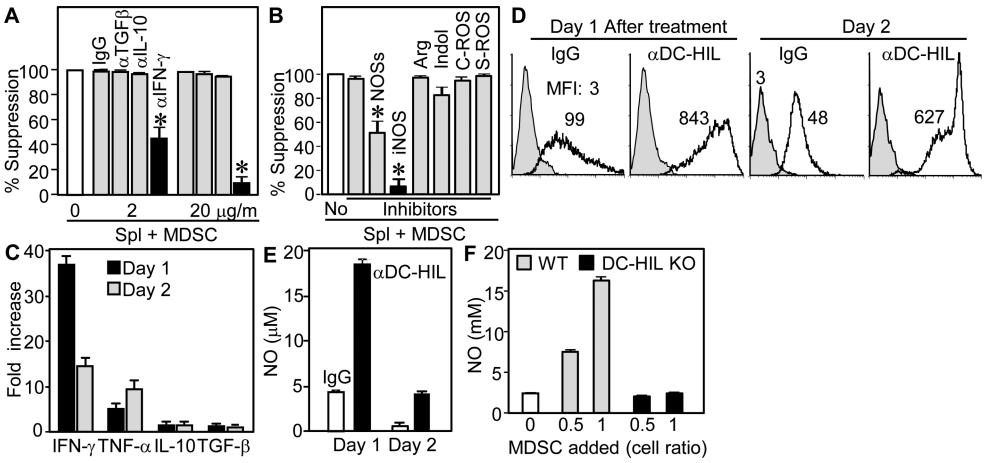

Figure 7. Activation of DC-HIL on MDSC induced expression of IFN-γ, NO, and ROS

(**A** and **B**) Specific inhibitors were added separately to cocultures of spleen cells and MDSC (1:1 cell ratio) isolated from EAE-sick mice; including anti-cytokine Ab (**A**) and 5 mM L-NG-monomethyl-arginine citrate (inhibitor for NOSs); 0.5 mM N6-(1-iminoethyl)-L-lysine (iNOS); 1 mM N-hydroxyl-nor-arginine (Arg); 0.2 mM 1-methyl-tryptophan (Indol); 1,000 U/ml catalase (C-ROS); and 200 U/ml superoxide dismutase (S-ROS). Effects of inhibitors are expressed as % suppression relative to untreated coculture (set as 100%). (**C** through **E**) One or 2 days after culturing MDSC with immobilized anti-DC-HIL mAb or control IgG, cytokine secretion (**C**), ROS expression (**D**) and NO production (**E**) were measured by the cells. Cytokine expression is shown by fold increase relative to IgG-treated cultures. ROS expression is shown in gray-filled (untreated MDSC) or open (Ab-treated) histograms, with mean fluorescence intensity (MFI). (**F**) Varying doses of MDSC from EAE-sick WT or DC-HIL$^{-/-}$ mice were added to spleen cell culture, and NO levels measured.

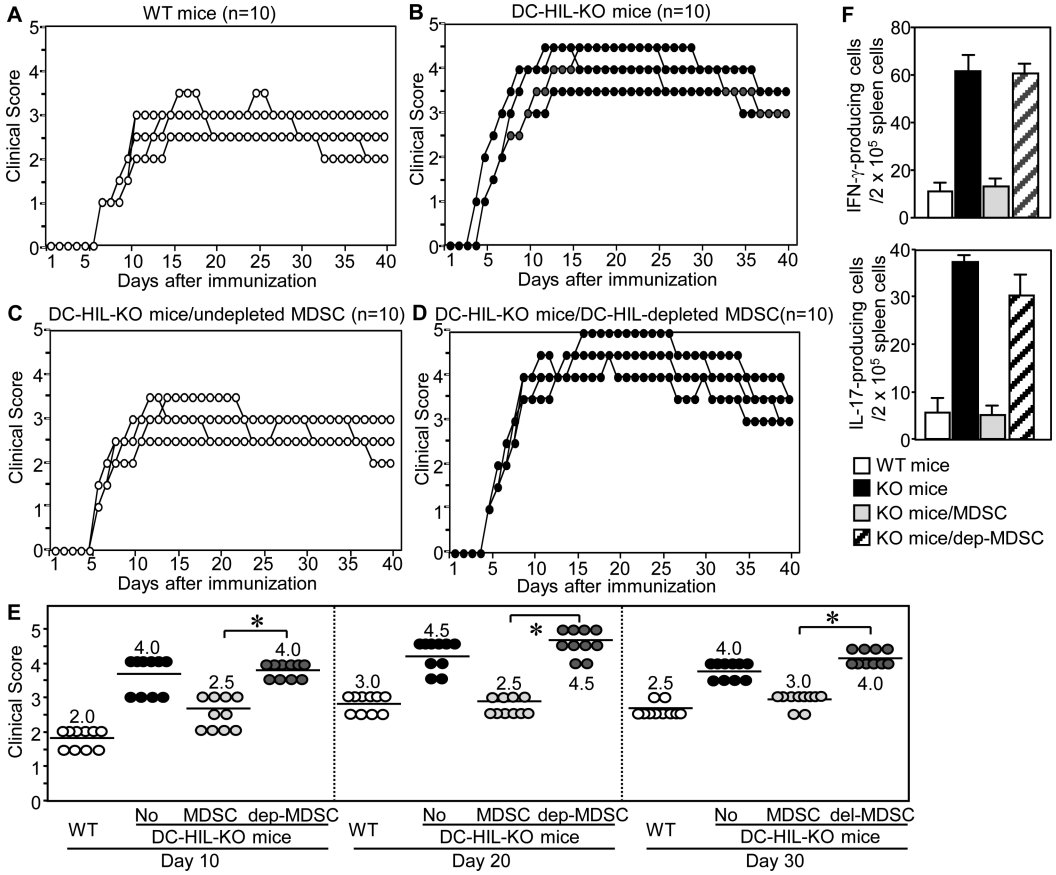

Figure 8. Adoptively transferred DC-HIL$^+$ MDSC reduced severity of EAE in DC-HIL KO mice

MDSC were isolated from EAE-sick WT mice (day 10 after EAE-immunization) and undepleted (MDSC) (**C**) or depleted of DC-HIL$^+$ cells (dep-MDSC) (**D**) and adoptively transferred into DC-HIL KO mice (n=10) on day 4 after EAE-immunization. In the same experiment, WT (**A**) or KO (**B**) mice without injections served as controls. (**E**) Each clinical score on early- (day 10), mid- (day 20) or late-phase (day 30) was plotted in a scatter chart (median) with statistical significance (*p<0.001) of scores between mice with undepleted and depleted MDSC. "No" means mice without cell infusions. (**F**) In separate experiments, the same panels (n=4) were treated similarly: on day 10 after immunization, all mice were examined for IFN-γ- or IL-17-producing cells in their spleens and calculated as the number per 2 x 10^5 spleen cells (mean ± sd, n=4). p<0.001 between mice with undepleted and depleted MDSC. Data are representative of 3 (**A** through **E**) and 2 (**F**) independent experiments.